Oncogene (2015) **34,** 878–889

www.nature.com/onc

ORIGINAL ARTICLE

SAA1 polymorphisms are associated with variation in antiangiogenic and tumor-suppressive activities in nasopharyngeal carcinoma

HL Lung[1], OY Man[1], MC Yeung[1], JMY Ko[1], AKL Cheung[1], EWL Law[1], Z Yu[1], WH Shuen[1], E Tung[1,2], SHK Chan[1], DK Bangarusamy[3,8], Y Cheng[1], X Yang[1], R Kan[1], Y Phoon[1], KC Chan[1], D Chua[1,2,4], DL Kwong[1,2], AWM Lee[2,5,6], MF Ji[7] and ML Lung[1,2]

Nasopharyngeal carcinoma (NPC) is a cancer that occurs in high frequency in Southern China. A previous functional complementation approach and the subsequent cDNA microarray analysis have identified that *serum amyloid A1* (*SAA1*) is an NPC candidate tumor suppressor gene. SAA1 belongs to a family of acute-phase proteins that are encoded by five polymorphic coding alleles. The *SAA1* genotyping results showed that only three *SAA1* isoforms (*SAA1.1*, *1.3* and *1.5*) were observed in both Hong Kong NPC patients and healthy individuals. This study aims to determine the functional role of *SAA1* polymorphisms in tumor progression and to investigate the relationship between *SAA1* polymorphisms and NPC risk. Indeed, we have shown that restoration of *SAA1.1* and *1.3* in the *SAA1*-deficient NPC cell lines could suppress tumor formation and angiogenesis *in vitro* and *in vivo*. The secreted SAA1.1 and SAA1.3 proteins can block cell adhesion and induce apoptosis in the vascular endothelial cells. In contrast, the SAA1.5 cannot induce apoptosis or inhibit angiogenesis because of its weaker binding affinity to αVβ3 integrin. This can explain why *SAA1.5* has no tumor-suppressive effects. Furthermore, the NPC tumors with this particular *SAA1.5/1.5* genotype showed higher levels of *SAA1* gene expression, and *SAA1.1* and *1.3* alleles were preferentially inactivated in tumor tissues that were examined. These findings further strengthen the conclusion for the defective function of *SAA1.5* in suppression of tumor formation and angiogenesis. Interestingly, the frequency of the *SAA1.5/1.5* genotype in NPC patients was ~2-fold higher than in the healthy individuals ($P = 0.00128$, odds ratio = 2.28), which indicates that this *SAA1* genotype is significantly associated with a higher NPC risk. Collectively, this homozygous *SAA1.5/1.5* genotype appears to be a recessive susceptibility gene, which has lost the antiangiogenic function, whereas *SAA1.1* and *SAA1.3* are the dominant alleles of the tumor suppressor phenotype.

Oncogene (2015) **34,** 878–889; doi:10.1038/onc.2014.12; published online 10 March 2014

INTRODUCTION

Nasopharyngeal carcinoma (NPC) is a squamous cell carcinoma originating from the epithelial cells around the nasopharynx. NPC has a high incidence in Southern China and Southeast Asia, but is rare in most Western countries,[1–4] suggesting there may be a genetic predisposition to NPC. We have previously used a functional complementation approach to generate chromosome 11 microcell hybrids (MCHs) after the transfer of an additional intact chromosome 11.[5] The current oligonucleotide microarray profiling of tumor-suppressive MCHs versus the tumorigenic recipient NPC cell line and tumorigenic revertants identified an interesting differentially expressed gene, *serum amyloid A1* (*SAA1*), as a candidate gene.

SAA encodes an acute-phase high-density lipoprotein-associated apolipoprotein, whose levels are greatly elevated following injury, inflammation and cancer.[6] It has been reported that *SAA1* is involved in several functions, which include induction of extracellular matrix-degrading enzymes for tissue repair,[7,8] recruitment of immune cells to inflammation sites[9–11] and lipid transport and metabolism.[12–16] SAA is a generic term for a family of acute-phase proteins encoded by various *SAA* genes with a high genetic variation. The human *SAA1*, *2*, *3* and *4* genes map in a 150 kb region of chromosome 11p15.1.[17] *SAA1* has five polymorphic alleles, *SAA1.1*, *SAA1.2*, *SAA1.3*, *SAA1.4* and *SAA1.5*, encoding distinct proteins with a few amino-acid differences (Figure 1a). The *SAA1* polymorphisms have been reported as risk factors in certain inflammatory diseases. However, how each *SAA1* variant is associated with NPC development remains unknown. In the present study, three *SAA1* allelic variants, *SAA1.1*, *1.3 and 1.5*, were identified in NPC patients and healthy Chinese individuals (Figure 1b). We compared the genotypes and allelic frequencies between the NPC patients and healthy individuals.

SAA has been identified as a serum biomarker in many different tumors,[18,19] including NPC.[20,21] The elevated serum SAA level might not be directly associated with early NPC tumor lesions, but could be a secondary product produced by the hepatocytes.[20] Our gene and protein expression analyses clearly showed that indeed *SAA1* was consistently downregulated in most tumorigenic NPC

[1]Department of Clinical Oncology and Center for Cancer Research, University of Hong Kong, Pokfulam, Hong Kong (SAR), People's Republic of China; [2]Center for Nasopharyngeal Carcinoma Research, University of Hong Kong, Hong Kong (SAR), People's Republic of China; [3]Genome Institute of Singapore, Biomedical Sciences Institutes, Singapore; [4]Comprehensive Oncology Centre, Hong Kong Sanatorium and Hospital, Happy Valley, Hong Kong (SAR), People's Republic of China; [5]Department of Clinical Oncology, Pamela Youde Nethersole Eastern Hospital, Hong Kong (SAR), People's Republic of China; [6]Department of Clinical Oncology, The University of Hong Kong-Shenzhen Hospital, Shenzhen, People's Republic of China and [7]Cancer Center, Zhongshan City Hospital, Zhongshan, People's Republic of China. Correspondence: Dr HL Lung or Professor ML Lung, Department of Clinical Oncology and Center for Cancer Research, University of Hong Kong, L6-02, Faculty of Medicine Building, 21 Sassoon Road, Pokfulam, Hong Kong (SAR), People's Republic of China. E-mail: hllung2@hku.hk or mlilung@hku.hk
[8]Current address: SciGenom Labs , Plot 43A, SDF 3rd Floor CSEZ, Kakkanad, Cochin, Kerala, 682037, India
Received 8 September 2013; revised 30 January 2014; accepted 31 January 2014; published online 10 March 2014

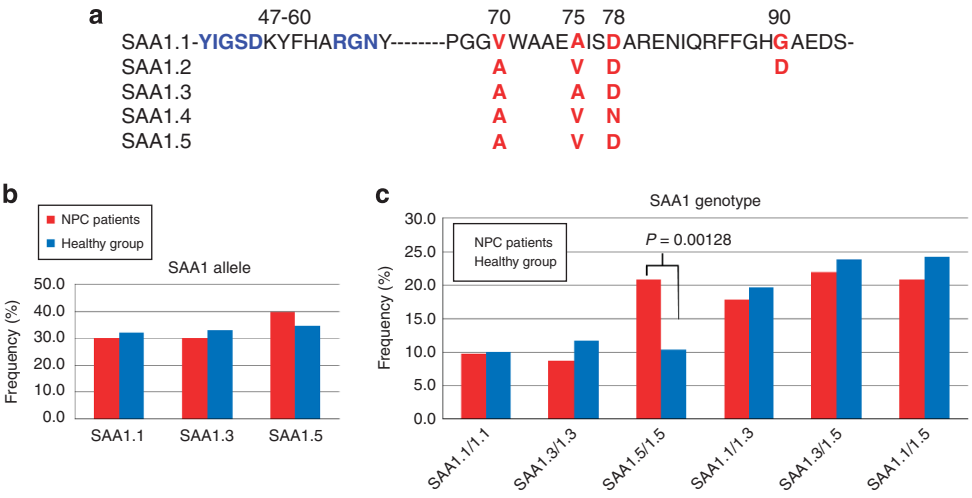

Figure 1. Disproportionate frequency of homozygous SAA1.5/1.5 in NPC patients. (**a**) The amino-acid differences among the five *SAA1* isoforms (*SAA1.1*, *1.2*, *1.3*, *1.4* and *1.5*.) The five human SAA1 proteins are distinguished by several amino-acid changes at positions 70, 75, 78 and 90, and are highlighted in red. The YIGSR- and RGD-like motifs are highlighted in blue. Comparisons of *SAA1* (**b**) alleles and (**c**) genotypes between NPC patients ($n = 196$) and healthy groups ($n = 289$). *SAA1.1*, *1.3* and *1.5* alleles were present in the NPC patients and healthy Hong Kong Chinese. The frequency of *SAA1.5/1.5* genotype in NPC patients was ~2-fold higher than in the healthy group (*P*-value = 0.00128, χ^2-test).

cell lines and tumor tissues. These results suggest that the physiological levels of *SAA1* expressed locally in the normal nasopharyngeal tissue might have a novel protective role against tumor development. In addition, both functional YIGSR- and RGD-like motifs are present in the SAA protein within close proximity (YIGSDKYFHARGNY; residues 47–60) (Figure 1a),[22] and proteins with YIGSR- and/or RGD-like motifs can inhibit angiogenesis, tumor cell adhesion to extracellular matrix, tumor growth and metastasis.[23–25] We examined the role of *SAA1.1*, *1.3 and 1.5* variants in inhibition of angiogenesis and involvement in tumor growth in NPC and investigated whether their biological activities would be distinguishable and be specifically associated with the risk, as observed in the *SAA1* genotyping analysis of the NPC patients.

RESULTS

SAA1 was differentially expressed in tumorigenic and tumor-suppressive cell lines

Suppression of tumorigenicity in the NPC HONE1 cells was observed after the transfer of an additional intact human chromosome 11 in the MCHs. The tumor segregants (TSs) are cell lines derived from tumors arising after a prolonged latency period after MCH inoculation in nude mice.[5] The tumor appearance may be associated with loss or inactivation of wild-type tumor suppressor genes originally present on the intact normal donor chromosome 11.[26] By using a 19 K oligonucleotide microarray, *SAA1* was also shown to be differentially expressed in comparative analysis of the chromosome 11 MCHs and TSs (Figure 2a). Genes upregulated in MCHs after chromosome transfer and downregulated in the TSs are presumably putative tumor suppressor genes.[27] Under the above criteria, *SAA1*, located at 11p15.1, was found to be the most differentially expressed gene (Figure 2b and Supplementary Table S1). The *SAA1* gene and the secreted SAA protein expression was verified by reverse transcription–polymerase chain reaction (RT–PCR) and western blot analyses and a good correlation was demonstrated (Figure 2c). In addition, from microarray analysis of the gene expression profile of four NPC cell lines (HONE1, HK1, CNE1, C666) versus the immortalized nasopharyngeal epithelial cell line NP460 (non-tumorigenic),[28] *SAA1* ranks the 7th most frequently downregulated genes (out of the 19 K genes) in the selected NPC cell lines (Supplementary Figure S1 and Supplementary Table S2). The frequencies and fold changes of downregulation and gene expression of other family members such as *SAA2* and *SAA4* were not as high as the *SAA1* (Supplementary Tables S1 and S2 and Supplementary Figures S2 and S3); *SAA3* is a pseudogene.[17] As a result, *SAA1* was chosen for further analysis.

Gene silencing of *SAA1* in NPC cell lines and tumors

The *SAA1* gene expression was frequently downregulated in NPC cell lines (6/7 = 85.7%) (Figure 2d) and tumor biopsies (39/57 = 68.4%) (Figure 3a). The *SAA1* gene silencing was attributed to promoter hypermethylation, as indicated by the bisulfite genomic sequencing (BGS) and the demethylation analyses (Figures 2e and f). As shown by the immunohistochemistry analysis of the NPC tissue microarray (TMA), the SAA protein was found primarily in the extracellular matrix and cytoplasm in the normal nasopharyngeal mucosae (Figure 3b). In the Zhongshan NPC cohort, reduced staining of SAA was observed in 28/31 (90.3%, *P*-value = 0.0025) informative NPCs (Figure 3c). In the Hong Kong cohort with more informative samples, the average intensity of the early NPC (T1/T2) primary tumors is significantly higher than the late-stage NPC tumors (*P*-value = 0.0018; Figures 3d and e). The current data suggest that the 'normal' physiological or the basal level of SAA1 in the epithelium may have an important role in cancer development.

Disproportionate frequency of homozygous *SAA1.5/1.5* in NPC patients versus healthy individuals and its association with higher gene expression levels in NPC tumors

To study the relationship between the *SAA1* allelic variants and NPC risk, the allelic frequencies of *SAA1* isoforms in NPC patients and healthy Chinese people were investigated by direct DNA sequencing. A total of 196 Hong Kong NPC patients and 289 healthy individuals were included in this *SAA1* genotyping study. Only *SAA1.1*, *1.3* and *1.5* were observed in both NPC patients and healthy individuals, whereas *SAA1.2 and 1.4* were not detected (Figure 1b and Supplementary Table S3). When the *SAA1* genotypes of the NPC group versus the healthy group were compared, the current results showed that the frequency of the *SAA1.5/1.5* genotype in NPC patientswas ~2-fold higher

(*P*-value = 0.00128) (Figure 1c). The *P*-value of this disproportionate frequency of *SAA1.5/1.5* genotype between the disease and healthy groups is statistically significant with >99% statistical power. When tumor *SAA1* gene expression levels of the six *SAA1* genotypes were analyzed (Supplementary Table S4), we found that the frequency of *SAA1.5/1.5* with high levels of *SAA1*

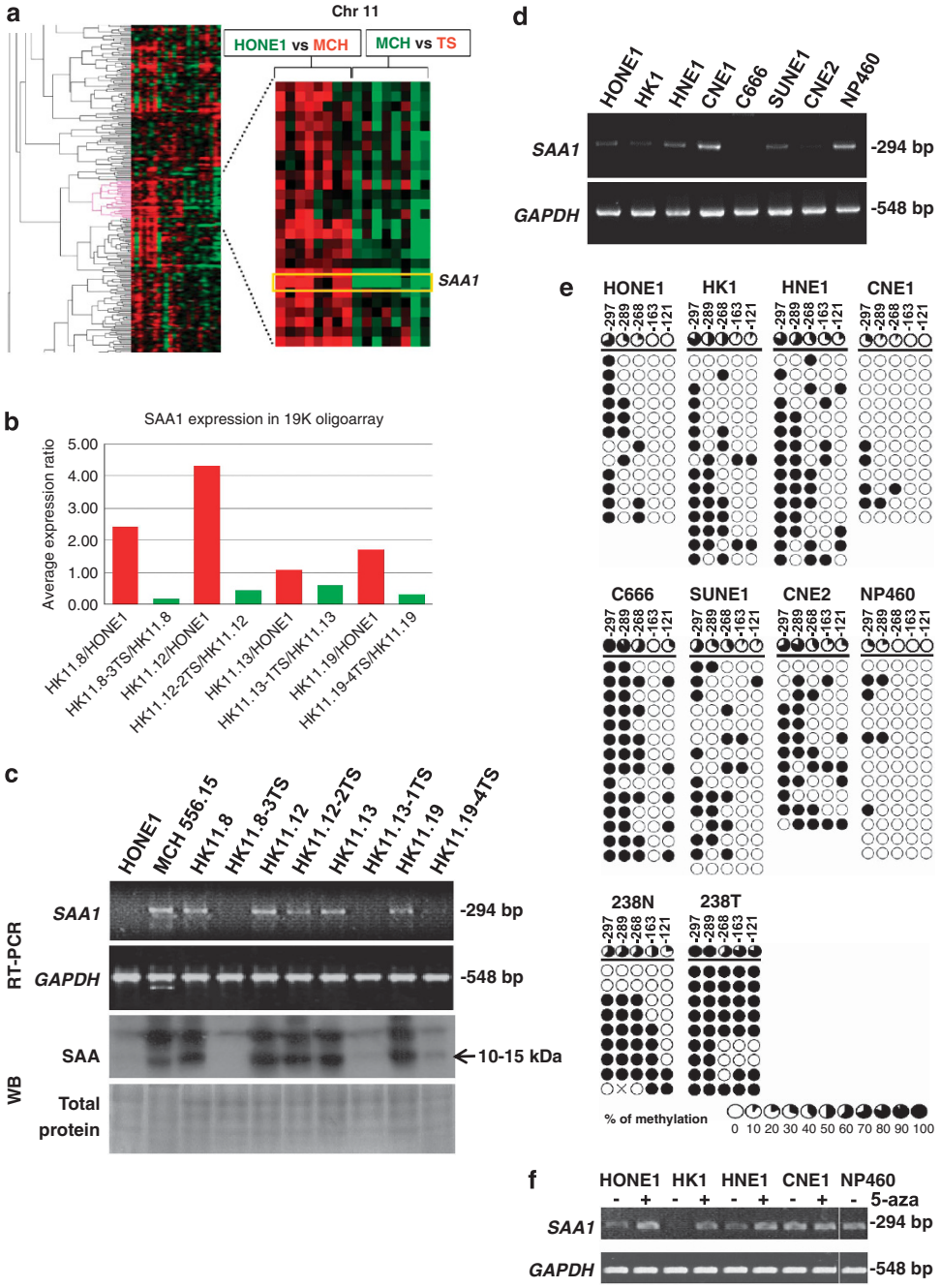

Figure 2. *SAA1* is differentially expressed in the tumor-suppressive MCHs against their matched TSs and is frequently downregulated in NPC cell lines and biopsies. (**a**) The heat map of the chromosome 11 19 K oligomicroarray results shows that the *SAA1* expression is differentially expressed in MCHs and their matched TSs. Red, upregulated expression; green, downregulated expression. (**b**) Microarray detection of *SAA1* in HONE1 versus MCHs (HK11.8, HK11.12, HK11.13, HK11.19) and the same MCHs versus their TSs (HK11.8-3TS, HK11.12-2TS, HK11.13-1TS, HK11.19-4TS). (**c**) The *SAA1* gene and protein expression in HONE1, MCH556.15, the four MCH cell lines and their TSs mentioned in (**b**). The gene expression was verified by RT–PCR. *GAPDH* was used as an internal control. The expression of the secreted SAA protein in the conditioned media was detected by western blot (WB) analysis. Coomassie blue staining was used to indicate equal loading of total protein in the conditioned media. (**d**) The *SAA1* gene expression in seven NPC cell lines. *GAPDH* was used as an internal control. NP460 cells were used as a normal control. (**e**) BGS analysis of five CpG sites in SAA1 promoter region of seven NPC cell lines (HONE1, HK1, HNE1, CNE1, CNE2, C666, SUNE1), the immortalized NP460 cell line and one NPC tumor (T)/non-tumor (N) tissue pair (no. 238). Each row represents an individual allele and the circles represent a single CpG dinucleotide. The CpG sites −297, −289, −268, −163 and −121 are shown from left to right; unmethylation (○) and methylation (●) status of CpG sites are as indicated. ×, Methylation status not determined owing to nucleotide change to an 'A' at the CpG site. (**f**) Re-expression of *SAA1* in NPC cell lines after treatment with 5 μM 5-aza-2′-deoxycytidine (5-aza) was monitored by RT–PCR analysis. *GAPDH* served as an internal control. NP460 was used as normal controls for comparison.

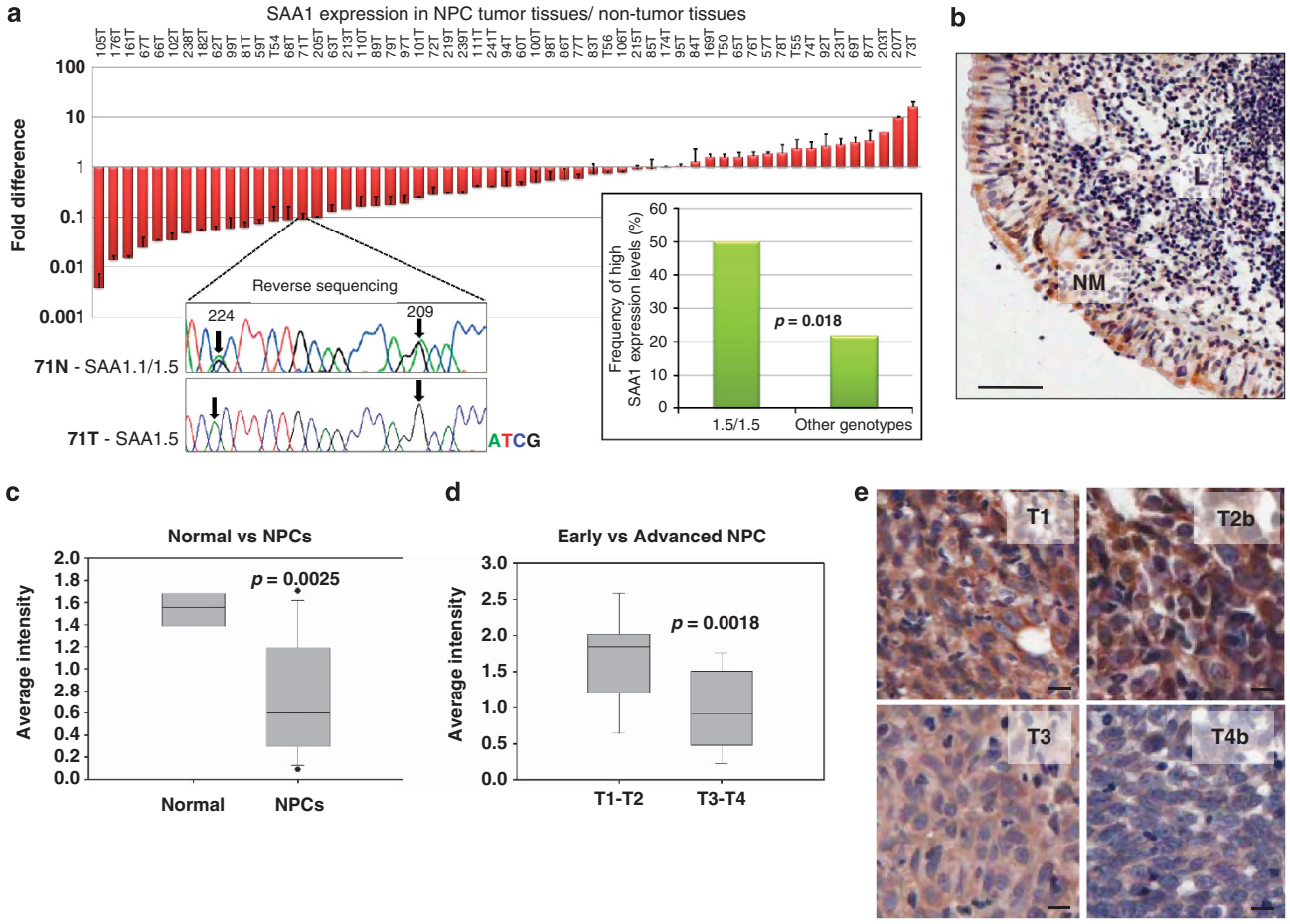

Figure 3. Clinical relevance of *SAA1* gene and protein expression in NPC. (**a**) Quantitative PCR (Q-PCR) was performed with 57 pairs of NPC tissues to study the fold change of *SAA1* expression in normal versus tumor tissues; 39 of 57 (68.4%) tumor tissue samples showed downregulated *SAA1* expression. The bar chart shows mean fold change of *SAA1* expression ± s.e.m. The comparison of frequencies of *SAA1.5/1.5* tissue samples with high *SAA1* gene expression levels against the frequencies with other *SAA1* genotypes is shown in the lower right-hand corner. High levels of *SAA1* expression is defined as fold change ⩾1. Representative sequencing results of *SAA1* in tumor (T) versus non-tumor (N) RNA in the NPC patient no. 71. A complete loss of *SAA1.1* mRNA expression was observed in the tumor RNA, as indicated by the arrows (loss of G and A at nucleotide positions 224 and 209, respectively; Supplementary Figure S4A). Part of the 'reverse' sequencing results is shown for the RNA samples. (**b**) Immunohistochemical staining of SAA in a normal nasopharyngeal mucosa (NM) of the Zhongshan NPC TMA. The underlying lamina propria of a normal human nasopharynx contains dense aggregates of lymphoid tissue (L).[56] Scale bar = 50 μm. (**c**) Comparison of immunohistochemical staining of SAA in NPC tissues ($n = 31$) versus normal tissues ($n = 4$) in the Zhongshan NPC TMA by a box plot. The *P*-value was calculated by Student's *t* -test. ● = outliner. (**d**) Comparison of SAA staining in early- ($n = 11$) versus late- ($n = 24$) stage primary NPC tissues in Hong Kong NPC TMA by a box plot. The *P*-value was calculated by Student's *t*-test. (**e**) Representative results of SAA with a staining index more than 2 were observed in a T1 or a T2 NPC specimen. T3 and T4 NPC tumors showed downregulation of SAA expression with a staining index < 1. The intensity of staining was graded by an arbitrary scale that ranged from 0 to 3, representing negative ('0'), weak ('1'), moderate ('2') and strong ('3') staining, respectively, and the proportion of immunopositive cells of interest were calculated. Scale bar = 10 μm.

expression was more than twofold higher than for other *SAA1* genotypes (*P*-value = 0.018; Figure 3a). Interestingly, when compared with the matched non-tumor RNA samples, we found that the *SAA1.1* or *1.3* mRNA expression was completely lost in three tumor tissues (sample nos. 71, 79 and 95), whereas the *SAA1.5* expression was retained (Figure 3a, Supplementary Figure S4 and Supplementary Table S4). In contrast, the DNA levels remain unchanged in the available cases (Supplementary Figure S4). Epigenetic inactivation could have a role in the gene silencing of *SAA1.1* and *SAA1.3* alleles in these NPC tissues.

Tumor suppressor function of *SAA1* is isoform specific

To study the functional roles of the three *SAA1* isoforms in NPC development, *SAA1.1*, *1.3 and 1.5* were constitutively expressed in HONE1, HK1 and C666 cell lines. The mRNA of the three *SAA1* isoforms was expressed in similar levels in each NPC cell line and is comparable with the nasopharyngeal epithelial cell line NP460, which reflects the 'normal' physiological *SAA1* level (Figure 4a). Tumorigenicity was suppressed with similar kinetics by restoration of *SAA1.1* and *SAA1.3* in all three cell lines (Figure 4b and Supplementary Table S5). In contrast, the growth rates of the *SAA1.5*-expressing cells were not significantly different from the vector alone. To further confirm the tumor-suppressive effect of *SAA1* in NPC, the *SAA1* short hairpin RNA (shRNA) knockdown was performed for the tumor-suppressive HK11.8 and HK11.12 MCHs, which express high levels of *SAA1* gene expression (Figure 2c). The *SAA1* genotyping results show that HK11.8 and HK11.12 express *SAA1.3* after the chromosome transfer from the chromosome 11 donor cells MCH556.15 (which contains the *SAA1.3* locus on the exogenous human chromosome). Reduction of *SAA1.3* gene and protein expression was observed in the two MCH cell lines by *SAA1* shRNA 364 (Figure 4c). After the *SAA1* gene knockdown

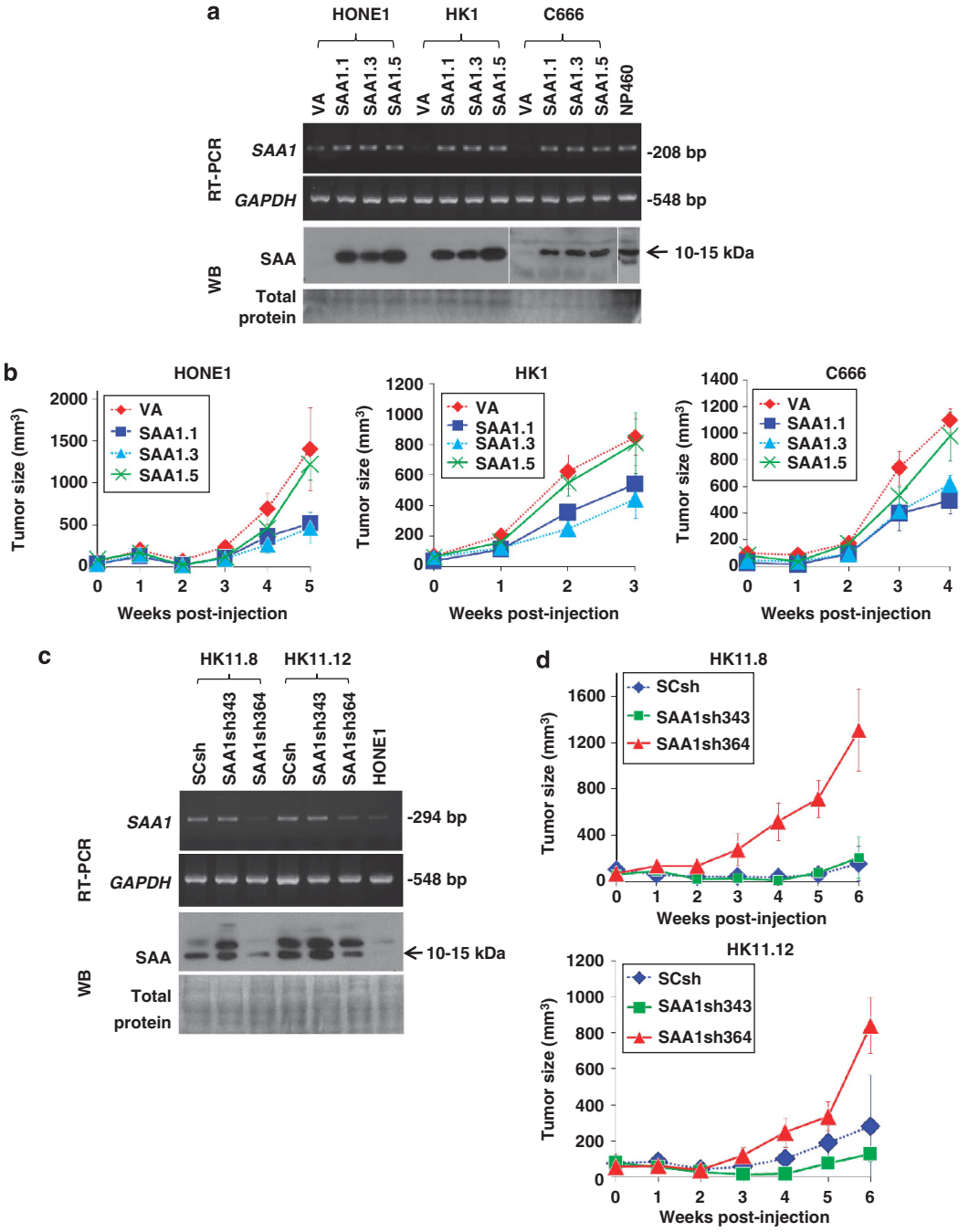

Figure 4. Tumor suppressor function of *SAA1* is isoform-dependent. (**a**) Restoration of *SAA1* gene and secreted SAA protein expression in the *SAA1.1*, *SAA1.3* and *SAA1.5* lentivirus-transduced NPC cell lines, as detected with semiquantitative RT–PCR and western blot analyses. NP460 was used as the normal *SAA1* level control. Total protein in the conditioned media was indicated by Coomassie blue staining. (**b**) The tumor growth curves for three *SAA1* variant-infected cell lines represent an average tumor volume of six injection sites inoculated for each cell population. Data are presented as the mean ± s.e.m. (**c**) Semiquantitative RT–PCR and western blot analyses of *SAA1* gene and secreted protein expression in the *SAA1*-knockdown MCHs. The two MCHs were stably infected with the *SAA1* shRNA oligonucleotides, SAA1shRNA343 and *SAA1*shRNA364. HONE1 cells served as a basal *SAA1* level control. Coomassie blue staining of total protein in the conditioned media was used to indicate equal loading. (**d**) Tumor growth kinetics of *SAA1*-knockdown MCHs versus the scramble controls. The tumor growth curves represent an average tumor volume ± s.e.m. of six sites. SCsh, scramble oligonucleotide control; VA, vector-lone; WB, western blot analysis.

by this shRNA, the tumorigenicity of both HK11.8 and HK11.12 was reversed (Figure 4d and Supplementary Table S5). For the shRNA343-infected cells, their tumor growth kinetics were not significantly altered. Thus, the secreted SAA1.1 and 1.3 protein levels are negatively correlated with the tumor formation capacity of the NPC cell lines.

SAA1.1 and *SAA1.3*, but not *SAA1.5*, inhibited *in vivo* and *in vitro* angiogenesis

To examine the role of *SAA1.1*, *1.3* and *1.5* variants in inhibition of angiogenesis, vascular endothelial cell tube formation and gel plug assays were performed. Both the *in vitro* and *in vivo* angiogenesis assay results showed that the *SAA1.5*-transduced cell

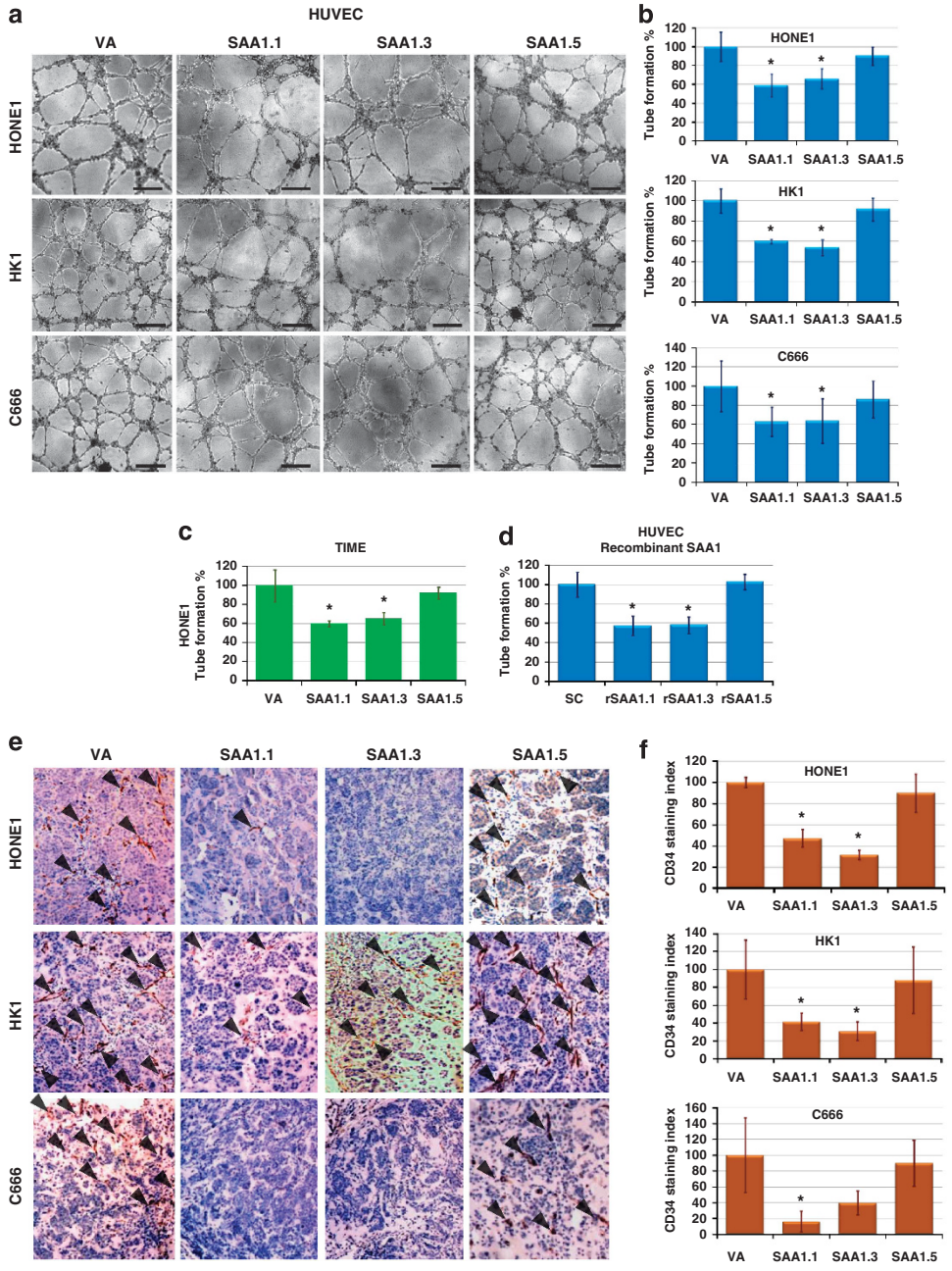

Figure 5. *SAA1.1* and *SAA1.3*, but not *SAA1.5*, inhibited *in vivo* and *in vitro* angiogenesis. (**a**) Representative results of the *in vitro* HUVEC tube formation assay after restoration of *SAA1.1*, *SAA1.3* and *SAA1.5* in the three NPC cell lines. Scale bar = 200 μm. (**b**) The percentage of HUVEC tube formation ability of three *SAA1* isoform-infected cells, as compared with their corresponding vector-alone controls. Data are presented as the mean ± s.e.m. of at least three independent experiments. *Statistically significant difference from the vector-alone clone ($P < 0.05$, Student's *t*-test). (**c**) The percentage of telomerase-immortalized human microvascular endothelial cell (TIME) tube formation ability of three *SAA1* isoform-infected HONE1 cells. Data are presented as the mean ± s.e.m. of four independent experiments. *$P < 0.05$, Student's *t*-test. (**d**) The percentage of HUVEC tube formation ability after treatment of SAA1.1, SAA1.3 and SAA1.5 recombinant proteins (20 μM) for 5 h. Data are presented as the mean ± s.e.m. *$P < 0.05$, Student's *t*-test. (**e**) Representative results from *in vivo* Matrigel plug assay in the *SAA1.1*, *SAA1.3* and *SAA1.5* lentivirus-transduced NPC cell lines. The endothelial cells were stained with anti-CD34 antibody, as indicated by arrows. Scale bar = 100 μm (**f**) CD34 staining index of the three *SAA1* variant-transduced NPC cells as compared with their corresponding vector-alone controls. Data are presented as the mean ± s.e.m of 4–5 gel plugs per cell line. *$P < 0.05$, Student's *t*-test. rSAA, recombinant SAA proteins; SC, solvent control.

lines could not significantly reduce the tube formation of the human umbilical vein endothelial cells (HUVECs) and telomerase-immortalized human microvascular endothelial cells (Figures 5a–c and Supplementary Figure S5) or the number of microvessels in the gel plugs (Figures 5e and f), whereas the *SAA1.1* and *1.3* substantially reduced the tube formation (34–46% inhibition) and the number of microvessels (53–76% inhibition). There was no significant effect on the number of viable cells after restoration of the three *SAA1* isoforms in the NPC cell lines (Supplementary Figure S6). The tumor suppression by *SAA1.1* and *1.3* is likely due to inhibition of angiogenesis. To ascertain the direct antiangiogenic activities of the SAA1 proteins, the

recombinant proteins of the three SAA1 isoforms were produced. An identical quantity (20 μM) of the three SAA variant proteins was used to treat the HUVECs. The SAA1.1 and SAA1.3 protein-treated samples showed the greatest suppression in the tube formation abilities (~40% inhibition), whereas the SAA1.5 treatment showed no reduction (Figure 5d). These results are consistent with the secreted SAA1.1 and 1.3 proteins being able to act directly on the vascular endothelial cells to suppress their tube formation.

SAA1.5 delayed the stress fiber formation and focal adhesions, but did not induce apoptosis of vascular endothelial cells

The integrin αVβ3 is a receptor for RGD-containing proteins and actively contributes to the regulation of tumor angiogenesis.[29,30] The current mechanistic study clearly shows that with the recombinant SAA1.5 protein there was a temporary delay in the assembly of integrin αVβ3-mediated focal adhesions and stress fiber of the HUVECs (1–6 h); the aberrant cell morphology was eventually restored at 24 h (Figure 6). In contrast, the SAA1.1- and 1.3-treated cells shrank with abolishment of formation of stress fiber and αVβ3 focal adhesions from 1 to 24 h (Figure 6) and the cells eventually underwent apoptosis with the decrease of viable cell numbers at 72 h (Figures 7a and b). In addition, when a high concentration of the αVβ3/β5 agonist (vitronectin) was added to the HUVECs, the effects of SAA1.1- and 1.3-induced apoptosis and disruption of focal adhesions were completely abolished (Figures 7c and d). Interestingly, the closely related αVβ5-mediated focal adhesions were undetectable in HUVECs despite any treatment (Supplementary Figure S7). At the molecular level, the focal adhesion kinase (FAK) phosphorylation (at residue Y397) was detected in the solvent control HUVECs and the SAA1.5-treated cells with weaker signal; however, activated FAK was barely detected in the HUVECs treated with SAA1.1 and 1.3 (Figure 7e). In contrast, the active caspase-3 was exclusively observed in HUVECs treated with these two SAA1 variant proteins. The co-immunoprecipitation results showed that the purified αVβ3 protein indeed could directly interact with the three SAA1 proteins. The interaction of SAA1.5 protein was weaker than the other two SAA1 proteins, when vitronectin was added (Figure 7f). Indeed, the integrin-binding assay results show that the SAA1.1, 1.3 and 1.5 proteins could displace the competing binding ligand (vitronectin) with IC_{50} (half-maximal inhibitory concentration) values of 0.26, 0.32 and 0.78 μM, respectively. It is likely that the SAA1.1 and 1.3 proteins are more effective in inhibiting the assembly of focal adhesion and stress fiber by directly blocking the integrin αVβ3 on HUVECs.

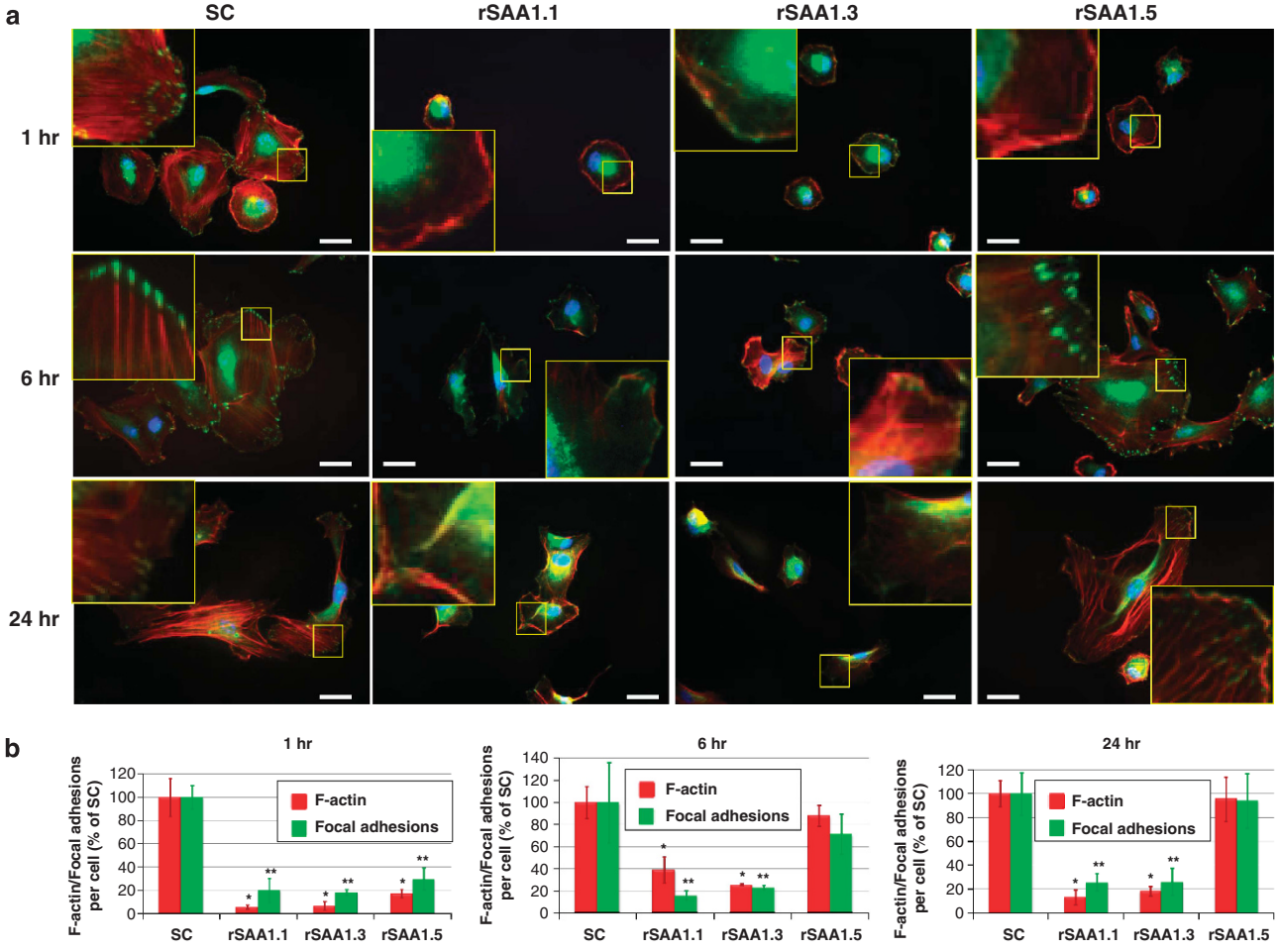

Figure 6. The SAA1.5 protein delayed the assembly of stress fiber and focal adhesions. (**a**) Representative fluorescent images of the effects of the SAA1.1, 1.3 and SAA1.5 (25 μg/cm^2) on remodeling of actin cytoskeleton and focal adhesions of HUVECs on vitronectin (0.25 μg/cm^2) from 1 to 24 h. Stress fibers (red) and focal adhesions (green solid spots) were stained with rhodamine phalloidin and anti-αVβ3 integrin antibody, respectively. Fluorescence images are enlarged in the yellow boxes to show the F-actin and focal adhesion staining. The nuclei were stained with 4,6-diamidino-2-phenylindole (DAPI, blue). Scale bar = 4 μm. (**b**) Analyses of formation of stress fibers and focal adhesions in HUVECs after treatment with the three SAA1 proteins from 1 to 24 h. Data are presented as the mean ± s.e.m. *Statistically significant difference of stress fiber formation from the solvent control (SC), **Statistically significant difference of focal adhesions from the SC ($P < 0.05$, Student's *t* -test). rSAA, recombinant SAA proteins.

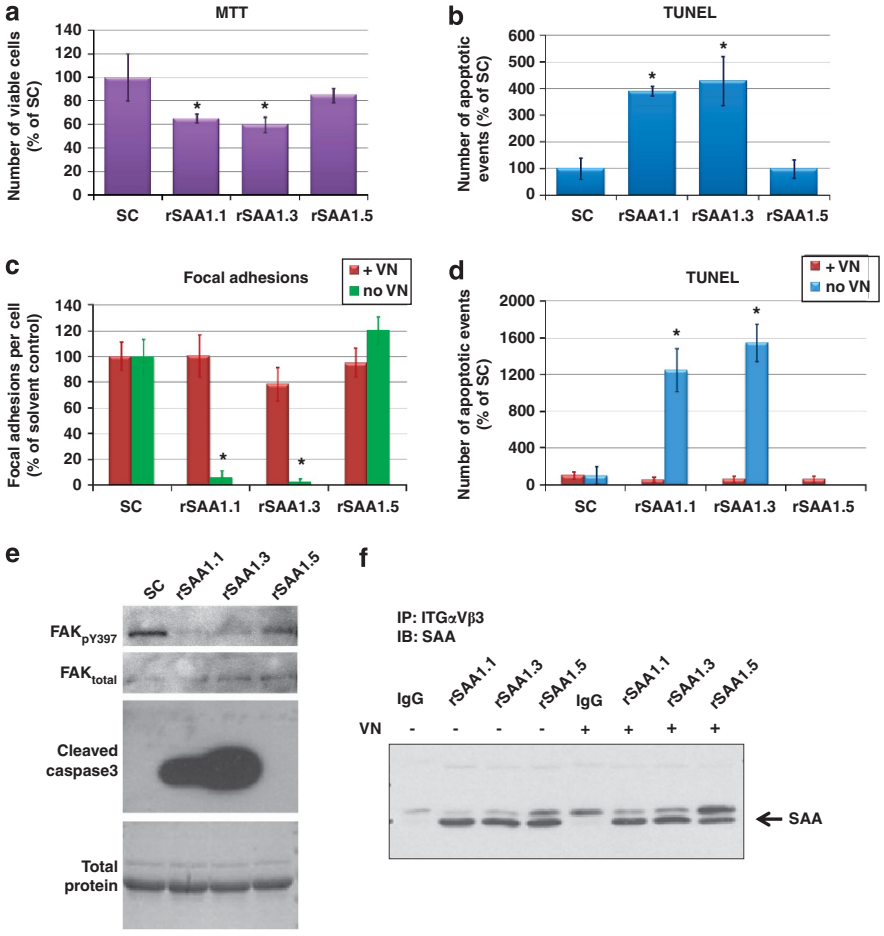

Figure 7. The SAA1.1 and 1.3 proteins induced the integrin blockade in HUVECs. (**a**) The number of viable HUVECs after the recombinant SAA1 protein treatments (25 μg/cm^2) for 72 h. MTT (3-[4,5-dimethylthiazol-2-yl]-2,5 diphenyl tetrazolium bromide) assay was performed to determine the number of viable cells. Data are presented as the mean ± s.e.m. *$P < 0.05$, Student's *t* -test. (**b**) The number of apoptotic cells in the SAA1.1, 1.3 and 1.5 protein-treated HUVECs for 48 h. Apoptosis of HUVECs after the recombinant SAA1 protein treatments (25 μg/cm^2) was detected by the terminal deoxynucleotidyl transferase dUTP nick-end labeling (TUNEL) assay. Data are presented as the mean ± s.e.m. *$P < 0.05$, Student's *t* -test. (**c**) Analyses of formation of focal adhesions in HUVECs after treatment with the three SAA1 proteins (25 μg/cm^2) in the presence or absence high concentration of VN (5.4 μg/cm^2) for 2 h. Data are presented as the mean ± s.e.m. *Statistically significant difference from the solvent control (SC) ($P < 0.05$, Student's *t* -test). VN, vitronectin. (**d**) The number of apoptotic cells in the SAA1.1, 1.3 and 1.5 protein-treated HUVECs in the presence of high concentration of VN for 72 h. Apoptosis of HUVECs after the recombinant SAA1 protein treatments (25 μg/cm^2) ± VN (5.4 μg/cm^2) was detected by the TUNEL assay. Data are presented as the mean ± s.e.m. *$P < 0.05$, Student's *t*-test. (**e**) Western blot analysis of phosphorylated-focal adhesion kinase (FAK) (at Y397), total FAK and activated caspase-3 in HUVEC cells treated by SAA1.1, 1.3 and 1.5 proteins (25 μg/cm^2) for 1 h. Coomassie blue staining of total protein in the cell lysates was used to indicate equal loading. (**f**) The SAA1 proteins are associated with the αVβ3 integrin protein as shown by co-immunoprecipitation (IP) assay. The recombinant αVβ3 integrin (1 μg) and SAA1 proteins (1 μg) in the presence or absence of VN (1 μg) were precipitated with antibody against αVβ3, or with purified immunoglobulin G (IgG) control, followed by immunoblotting (IB) with the SAA antibody. rSAA, recombinant SAA proteins.

DISCUSSION

Although SAA is well known as an acute-phase protein and is produced in the liver in response to a variety of stimuli, the current data suggest that the 'normal' physiological or the basal level of SAA1 in the epithelium may have an important different role in cancer development. Indeed, the SAA expression was shown to be predominantly expressed in the epithelia of many histologically normal human tissues.[31,32] In a number of cancer tissues, SAA protein expression was almost undetectable or reduced as compared with their normal counterparts.[32] With the transfer of an intact chromosome 11 or lentiviral infection of *SAA1*, the physiological level of *SAA1* can be restored in the *SAA1*-deficient NPC cell lines. Restoration of the *SAA1.1* and *SAA1.3* in the NPC cell lines can effectively suppress tumor formation and angiogenesis *in vitro* and *in vivo*; the knockdown of *SAA1.3* in the *SAA1*-expressing MCHs can initiate tumor formation.

Surprisingly, the constitutively expressed *SAA1.5* is defective in tumor suppression and inhibition of angiogenesis. In agreement with these findings, tumors with *SAA1.5/1.5* genotype expressed higher *SAA1* gene expression levels, whereas the *SAA1.1* and *1.3* alleles seem to be preferentially inactivated in some NPC tissues by an epigenetic mechanism. Interestingly, when we genotyped the *SAA1* polymorphisms in NPC patients versus the healthy individuals, we showed that the probability of the *SAA1.5/1.5* genotype occurring in the NPC group is ~2.3 times greater than the probability of this genotype occurring in the healthy individuals (odds ratio = 2.28); individuals having the *SAA1.5/1.5* genotype would be ~1.5 times as likely as genotypes other than *SAA1.5/1.5* to develop NPC (relative risk = 1.54). This suggests that individuals harboring the *SAA1.5/1.5* homozygous genotype are more susceptible to develop NPC. To our knowledge, this is the first report to describe the preferential association of *SAA1* variants with cancers.

The current mechanistic study clearly shows that with the SAA1.5 protein, there is a temporary delay in the assembly of stress fiber and integrin αVβ3-mediated focal adhesions of the HUVECs; the aberrant cell morphology is eventually restored. In contrast, the fate of the SAA1.1 and 1.3 treatments differ; the cells shrank (because of disruption of focal adhesions and stress fiber formation) and underwent apoptosis in an integrin αVβ3-dependent manner as a likely consequence of loss of cell contact with the extracellular matrix induced by the integrin blockade by these two SAA1 proteins and resulting in a type of caspase-dependent apoptosis known as anoikis.[33] This observation can be attributed to the lowest affinity of the SAA1.5 protein for the integrin αVβ3 among the three SAA1 isoforms identified in the present study. The present study clearly showed that the SAA1.1 and SAA1.3 proteins are antiangiogenic proteins, which strongly bind to integrin αVβ3 to abolish the stress fiber assembly and focal adhesions of the vascular endothelial cells. Structurally, the major differences among these three SAA1 isoforms lies in the variant amino acids located at positions 70 and 75, which are not located within the RGD- and YIGSR-like motifs (Figure 1a). This change may affect the exposure of these implicit functional motifs and contributes to the variations in the biological activities among the three SAA1 isoforms. Collectively, we clearly show that the *SAA1.5* variant is a defective form of the family with respect to its antiangiogenic phenotype, whereas *SAA1.1* and *SAA1.3* are the dominant functional alleles. As a result, the homozygous *SAA1.5-/1.5* genotype is likely to be a recessive susceptibility genotype, which is supported by the higher occurrence of *SAA1.5/1.5* in the NPC patients, when compared with the healthy individuals.

In conclusion, the *SAA1.5/1.5* polymorphism represents one of the genetic predisposition factors that may be an identifier of those individuals at greater risk for NPC. The SAA protein is reported to be predominantly expressed in the normal epithelia of various tissues; thus, the *SAA1* genotypes may have some role in tumor development of other cancer types of epithelial origin. Will this particular *SAA1.5* variant alter other reported functions of SAA1 as an acute-phase protein? Apparently, the other two *SAA1* variants, *SAA1.2* and *SAA1.4*, are absent in the Hong Kong Chinese; what are their roles in angiogenesis and tumor development? As these two *SAA1* variants might be present in other ethnic groups, would their absence/presence in different populations have any role in the high NPC incidence rates in the endemic regions? This study of *SAA1* polymorphisms in NPC has opened up several new intriguing avenues for future investigations.

MATERIALS AND METHODS

Cell lines

Culture conditions for the NPC cell lines were as described.[28,34–36] The immortalized nasopharyngeal epithelial cell line NP460 was cultured as described.[28,37] The donor chromosome 11 cell line MCH556.15, the HONE1/chromosome 11 MCHs and their TSs were cultured as described.[5] HUVECs (Cascade Biologics, Portland, OR, USA) and telomerase-immortalized human microvascular endothelial cells (ATCC, Manassas, VA, USA) were cultured as described.[38,39] The immortalized esophageal epithelial cell lines, NE083 and NE1, were cultured as described.[40,41] All cell lines used in the current study were confirmed to be mycoplasma negative. The NPC cell lines were obtained from the Hong Kong NPC AoE Cell Line Repository (Pokfulam, Hong Kong) and have been authenticated.

Gene expression analysis using oligonucleotide microarray hybridization

The microarray preparation, the dye coupling and the subsequent hybridization were conducted, as described previously.[26]

Tissue specimens for *SAA1* gene expression analysis

For *SAA1* gene expression analysis, matched normal nasopharyngeal and NPC biopsies from 57 NPC patients were collected at Queen Mary Hospital in Hong Kong from 2006 to 2010, as described.[42] The study protocol was approved by the Hospital Institutional Review Board and written consents were obtained from all patients.

RT–PCR and quantitative PCR analyses

Semiquantitative and quantitative PCR were performed as reported.[43] The SAA1/2 primers, SAA1-RT-F1 and -R1 (for exogenous SAA1 expression), the SAA1-specific primers, SAA1-RT-F2 and -R2, and the glyceraldehyde 3-phosphate dehydrogenase (GAPDH) primers, GAPDH-RT-F1 and -R1, were used for semiquantitative RT–PCR (Supplementary Table S6). The SAA1 primers, SAA1-RT-F1 and -R2, and the GAPDH primers, GAPDH-RT-F2 and -R2 (Supplementary Table S6), were used for this quantitative PCR analysis.

Western blot analysis

Western blot analysis of SAA was performed as reported.[26] The SAA antibody (Abcam, Cambridge, UK) and Ab-1 (Calbiochem, Darmstadt, Germany) were used for the detection of SAA and α-tubulin, respectively. To our knowledge, the current SAA antibody and other commercial or non-commercial SAA antibodies are not able to distinguish the SAA1 from SAA2 protein. By convention, the word 'SAA' was used to describe the western blot results of the SAA1/2. Antibodies against FAK (pY397), FAK (total) and caspase-3 were supplied from Cell Signaling Technology (Danvers, MA, USA).

NPC TMAs

For construction of the two NPC TMAs, 45 NPC specimens were collected in Zhongshan City Hospital, Mainland China (Zhongshan NPC cohort), and 55 NPC specimens were collected in Queen Mary Hospital and Pamela Youde Nethersole Eastern Hospital, Hong Kong (Hong Kong NPC cohort). Details of the clinical information of the two TMAs are listed in Supplementary Table S7.

Immunohistochemical staining

Immunohistochemistry staining and analysis of the NPC TMAs were performed as described.[44] The rabbit anti-SAA polyclonal antibody (Santa Cruz Biotechnology, Santa Cruz, CA, USA) was used as the primary antibody. The SAA staining intensity was analyzed by Spectrum version 11.1.1.765 software (Aperio Technologies, Vista, CA, USA).

BGS analysis

The SAA1 promoter is identified based on previous studies.[45,46] The CpG sites of SAA1 in the promoter region were identified at the region from −1 to −390 bp across the transcription start sites (Supplementary Figure S8). The BGS primers were designed by MethPrimer (www.urgene.org/methprimer). A promoter region of 285 bp of the bisulfite-treated DNAs (Supplementary Figure S8) was amplified by SAA1-BGS-F and -R (Supplementary Table 6), and BGS for the amplified promoter regions was performed, as described previously.[47]

5-Aza-2′-deoxycytidine treatment

The NPC cell lines were treated with 5 μM 5-aza-2′-deoxycytidine (Sigma-Aldrich, St Louis, MO, USA) for 5 days before analysis, as described.[26]

DNA sequencing for *SAA1* genotyping

One hundred and thirty-one NPC tissues and 112 blood samples collected from 196 NPC patients and blood samples collected from 289 healthy individuals were used. Identical genotyping results were observed in 44 redundant blood and the matched tissue samples. For genotyping the tumor tissue samples, the cDNAs were used as templates for PCR reactions. PCR amplification was carried out with forward and reverse primers (*NheI*-SAA1-F and SAA1-RT-R2; Supplementary Table S6). The amplified *SAA1* cDNA fragments from clinical tissues were sequenced by using the reverse primer SAA1-RT-R2. The genomic DNA of the blood samples was used as templates for PCR reactions, and the template amplification with SAA1-RT-F1 and -R2 primers and DNA sequencing with SAA1-RT-F1 (Supplementary Table S6) primer were carried out.

Lentiviral vectors and infection for constitutive *SAA1* expression

The full open reading frames of *SAA1.1*, *1.3* and *1.5* were initially cloned into the pETE-Bsd vector[48] from cDNAs of cell lines NP460, MCH556.15 and

NE083, respectively, with *Nhe*I-SAA1-F and SAA1-*Bam*HI-rev primers (Supplementary Table S6). The full-length *SAA1.1*, *1.3* and *1.5* cDNAs were then subcloned into the lentiviral pWPI vector (Addgene plasmid 12254, Addgene, Cambridge, MA, USA) with *Pac*I-SAA1-F and SAA1-*Bam*H1-rev primers (Supplementary Table S6). The 293T cell line was transfected with the envelope and packaging vectors, pMD2.G and psPAX2 (Addgene plasmids 12259 and 12260), and expression vectors, pWP1-*SAA1.1*, -*SAA1.3*, -*SAA1.5*, or the vector alone. The NPC cells were transduced with filtered viral particles in the presence of 16 μg/ml polybrene. The infection efficiency was routinely >80% as demonstrated by the HONE1 cells (Supplementary Figure S9).

Knockdown of *SAA1* in chromosome 11 MCHs by lentiviral infection

The *SAA1* RNA knockdown was achieved by using the lentihair pLKO.1-TRC cloning vector (Addgene plasmid 10878).[49] In brief, two pairs of *SAA1* shRNA oligonucleotides (SAA1-shRNA343 and -shRNA364) were designed according to The RNAi Consortium (TRC) library (http://www.broad.mit.edu/genome_bio/trc/rnai.html). The sequences of the two oligonucleotide pairs and their target positions are shown in Supplementary Table S8. The shRNA oligonucleotides were ligated into a pLKO.1-TRC vector and the shRNA plasmids were transduced into the recipient cell lines 11.8 and 11.12, as described in the Addgene pLKO.1 Protocol (http://www.addgene.org/tools/protocols/plko/). The pLKO.1-scramble shRNA construct (Addgene plasmid 1864) was used as a negative control, as described previously[50] (the sequence is shown in Supplementary Table S8).

Tumorigenicity assay

Subcutaneous injection was performed, as described previously.[51]

Production and purification of recombinant SAA1 proteins

The synthesis of the SAA1 recombinant proteins was based on the method described by Yamada *et al.*[52] with some modifications. The pET-28a(+) (Novagen, Darmstadt, Germany) was used for recombinant His-tag SAA1 protein production. The three SAA1 isoforms with their signaling peptide sequence removed were amplified from plasmids of pETE-BSD-*SAA1.1*, *1.3* and *1.5* with Pet-*Nhe*1-SAA1F and SAA1-*Bam*H1-rev primers (Supplementary Table S6). Each PCR product was ligated to the pET-28a(+) vector. The cloned plasmids were transformed into *Escherichia coli* (BL21) and the protein expression was induced with isopropyl-β-D-thiogalactopyranoside (USB, Cleveland, OH, USA). The proteins were purified with the Ni-NTA agarose beads (Qiagen, Hilden, Germany) and were found to be at least 98% pure (Supplementary Figure S10). The endotoxin levels of the purified proteins were found to be < 0.003 endotoxin units (EU)/mg.

HUVEC and telomerase-immortalized human microvascular endothelial cell tube formation assays

The vascular endothelial cell tube formation was performed, as described previously.[43]

In vivo Matrigel plug angiogenesis assay

In vivo angiogenesis was studied by using the Matrigel plug assay, as described previously.[43]

MTT assay

The recombinant SAA1 proteins (25 μg/cm^2) were coated onto 96-well plates and then 1500 HUVECs were seeded on top. The MTT (3-[4,5-dimethylthiazol-2-yl]-2,5 diphenyl tetrazolium bromide) assay was performed, as described previously.[51]

Immunofluorescence staining of HUVECs

Vitronectin (0.25 μg/cm^2) (BD Biosciences, Le Pont de Claix, France) and the recombinant SAA1 proteins (25 μg/cm^2) were sequentially coated onto coverslips and immunofluorescence staining for stress fiber and focal adhesions in HUVECs was performed, as described previously.[53] The integrin-mediated focal adhesion was detected by using the αVβ3 or αVβ5 integrin primary antibody (Chemicon, Billerica, MA, USA). F-actin was stained with rhodamine phalloidin (Invitrogen, Carlsbad, CA, USA). Images were captured by an Olympus BX51 microscope (Olympus, Tokyo, Japan). The F-actin intensity and the number of focal adhesions were counted using Image J software (NIH, Bethesda, MD, USA).

Terminal deoxynucleotidyl transferase-mediated dUTP nick-end labeling assay

The terminal deoxynucleotidyl transferase dUTP nick-end labeling assay was performed by using an *in situ* Cell Death Detection Kit (Roche Diagnostics, Basel, Switzerland).

Co-immunoprecipitation

The co-immunoprecipitation assay was performed, as described previously.[44] In brief, 1 μg recombinant SAA1 protein was precleared with rProtein G Agarose (Invitrogen) and incubated with 1 μg purified recombinant human αVβ3 integrin (derived from CHO cells; R&D Systems, Minneapolis, MN, USA) and the mouse αVβ3 integrin antibody (0.8 μg; Chemicon) or the control purified mouse IgG (0.8 μg; Invitrogen), at 4 °C overnight. The protein mixtures were then immunoprecipitated with the rProtein G Agarose, washed and then subjected to western blot analysis.

Integrin-bindingactivity assay

In brief, 0.4 μg/ml of purified recombinant human αVβ3 integrin (derived from CHO cells; R&D Systems) was adsorbed onto a 96-well ELISA plate (Nunc, Roskilde, Denmark). The recombinant SAA1.1, 1.3 or 1.5 proteins were added to displace 0.25 μg/ml biotinylated vitronectin (Abcam) from the recombinant αVβ3 integrin. Detailed procedures of this ligand-binding assay and ligand-binding activities were evaluated, as described previously.[54] The integrin-binding results were expressed as IC_{50}s and were obtained after incorporating the data set of various SAA1 concentrations (0.03125 to 40 μg/ml) to a Sigmoid curve as described.[55]

Statistical analysis

The Student's *t*-test was performed for the functional assays for statistical comparison between the vector-alone and *SAA1*-expressing cells. Associations between clinical pathological information of NPC patients and gene and protein expression of *SAA1* were analyzed using SPSS11.0 statistics calculation software (SPSS Inc., Chicago, IL, USA). The association of *SAA1* genotypes with the NPC patients was analyzed by χ^2-test using Epi Info 7 statistical software (Centers for Disease Control and Prevention, Atlanta, GA, USA). The *P*-value of < 0.05 was considered statistically significant.

ABBREVIATIONS

ECM, extracellular matrix; MCH, microcell hybrid; NPC, nasopharyngeal carcinoma; SAA1, serum amyloid A1; TSG, tumor suppressor gene; TS, tumor segregant.

CONFLICT OF INTEREST

The authors declare no conflict of interest.

ACKNOWLEDGEMENTS

We acknowledge the AoE NPC Tissue Bank for providing the NPC specimens and the NPC TMA. We thank the Hong Kong Red Cross for providing us the blood from healthy individuals. We also thank Dr Edison Tak-Bun Liu for their microarray support in the Genome Institute of Singapore (GIS); Dr Sai Wah Tsao for providing us the immortalized cell lines; Dr John M Nicholls for the TMA analysis and Dr Pui Man Chiu for her help in constructing the NPC TMA and SAA immunohistochemistry staining; Dr Didier Trono for the supply of the lentiviral vectors, pWPI, pMD2.G and psPAX2. We thank Dr David Root for the supply of the lentihair pLKO.1-TRC cloning vector and Dr David Sabatini for the pLKO.1-scramble shRNA construct. This work was supported by the General Research Fund (HKU772309 to HLL) of the Research Grants Council of the Hong Kong Special Administrative Region.

REFERENCES

1 Wei WI, Sham JS. Nasopharyngeal carcinoma. *Lancet* 2005; **365**: 2041–2054.
2 Liu Q, Chen JO, Huang QH, Li YH. Trends in the survival of patientswith nasopharyngeal carcinoma between 1976 and 2005 in Sihui, China: a population-based study. *Chin J Cancer* 2013; **32**: 325–333.

3 Adham M, Kurniawan AN, Muhtadi AI, Roezin A, Hermani B, Gondhowiardjo S *et al*. Nasopharyngeal carcinomain Indonesia: epidemiology, incidence, signs and symptoms at presentation. *Chin J Cancer* 2012; **31**: 185–196.
4 Kataki AC, Simons MJ, Das AK, Sharma K, Mehra NK. Nasopharyngeal carcinomain the Northeastern states of India. *Chin J Cancer* 2011; **30**: 106–113.
5 Cheng Y, Stanbridge EJ, Kong H, Bengtsson U, Lerman MI, Lung ML. A functional investigation of tumor suppressor gene activities in a nasopharyngeal carcinoma cell line HONE1 using a monochromosome transfer approach. *Genes Chromosomes Cancer* 2000; **28**: 82–91.
6 Yamada T. Serum amyloid A (SAA): a concise review of biology, assay methods and clinical usefulness. *Clin Chem Lab Med* 1999; **37**: 381–388.
7 Mitchell TI, Coon CI, Brinckerhoff CE. Serum amyloid A (SAA3) produced by rabbit synovial fibroblasts treated with phorbol esters or interleukin 1 induces synthesis of collagenase and is neutralized with specific antiserum. *J Clin Invest* 1991; **87**: 1177–1185.
8 Strissel KJ, Girard MT, West-Mays JA, Rinehart WB, Cook JR, Brinckerhoff CE *et al.* Role of serum amyloid A as an intermediate in the IL-1 and PMA-stimulated signaling pathways regulating expression of rabbit fibroblast collagenase. *Exp Cell Res* 1997; **237**: 275–287.
9 Badolato R, Wang JM, Murphy WJ, Lloyd AR, Michiel DF, Bausserman LL *et al.* Serum amyloid A is a chemoattractant: induction of migration, adhesion, and tissue infiltration of monocytes and polymorphonuclear leukocytes. *J Exp Med* 1994; **180**: 203–209.
10 Preciado-Patt L, Hershkoviz R, Fridkin M, Lider O. Serum amyloid A binds specific extracellular matrix glycoproteins and induces the adhesion of resting CD4+ T cells. *J Immunol* 1996; **156**: 1189–1195.
11 Xu L, Badolato R, Murphy WJ, Longo DL, Anver M, Hale S *et al.* A novel biologic function of serum amyloid A. Induction of T lymphocyte migration and adhesion. *J Immunol* 1995; **155**: 1184–1190.
12 Cabana VG, Siegel JN, Sabesin SM. Effects of the acute phase response on the concentration and density distribution of plasma lipids and apolipoproteins. *J Lipid Res* 1989; **30**: 39–49.
13 Hoffman JS, Benditt EP. Secretion of serum amyloid protein and assembly of serum amyloid protein-rich high density lipoprotein in primary mouse hepatocyte culture. *J Biol Chem* 1982; **257**: 10518–10522.
14 Liang JS, Sipe JD. Recombinant human serum amyloid A (apoSAAp) binds cholesterol and modulates cholesterol flux. *J Lipid Res*, 1995; **36**: 37–46.
15 Liang JS, Schreiber BM, Salmona M, Gonnerman WA, de Beer FC, Phillip G *et al.* Amino terminal region of acute phase, but not constitutive, serum amyloid A (apoSAA) specifically binds and transports cholesterol into aortic smooth muscle and HepG2 cells. *J Lipid Res* 1996; **37**: 2109–2116.
16 Lindhorst E, Young D, Bagshaw W, Hyland M, Kisilevsky R. Acute inflammation, acute phase serum amyloid A and cholesterol metabolism in the mouse. *Biochim Biophys Acta* 1997; **1339**: 143–154.
17 Uhlar CM, Whitehead AS. Serum amyloid A, the major vertebrate acute-phase reactant. *Eur J Biochem* 1999; **265**: 501–523.
18 Malle E, Sodin-Semrl S, Kovacevic A. Serum amyloid A: an acute-phase protein involved in tumour pathogenesis. *Cell Mol Life Sci* 2009; **66**: 9–26.
19 Liu C. Serum amyloid a protein in clinical cancer diagnosis. *Pathol Oncol Res* 2012; **18**: 117–121.
20 Cho WC, Yip TT, Yip C, Yip V, Thulasiraman V, Ngan RK *et al.* Identification of serum amyloid a protein as a potentially useful biomarker to monitor relapse of nasopharyngeal cancer by serum proteomic profiling. *Clin Cancer Res* 2004; **10**: 43–52.
21 Liao Q, Zhao L, Chen X, Deng Y, Ding Y. Serum proteome analysis for profiling protein markers associated with carcinogenesis and lymph node metastasis in nasopharyngeal carcinoma. *Clin Exp Metastasis* 2008; **25**: 465–476.
22 Preciado-Patt L, Levartowsky D, Prass M, Hershkoviz R, Lider O, Fridkin M. Inhibition of cell adhesion to glycoproteins of the extracellular matrix by peptides corresponding to serum amyloid A. Toward understanding the physiological role of an enigmatic protein. *Eur J Biochem* 1994; **223**: 35–42.
23 Nicosia RF, Bonanno E. Inhibition of *angiogenesis invitro* by Arg-Gly-Asp-containing synthetic peptide. *Am J Pathol* 1991; **138**: 829–833.
24 Chiang HS, Yang RS, Huang TF. The Arg-Gly-Asp-containing peptide, rhodostomin, inhibits *in vitro* cell adhesion to extracellular matrices and platelet aggregation caused by saos-2 human osteosarcoma cells. *Br J Cancer* 1995; **71**: 265–270.
25 Iwamoto Y, Nomizu M, Yamada Y, Ito Y, Tanaka K, Sugioka Y. Inhibition of angiogenesis, tumour growth and experimental metastasis of human fibrosarcoma cells HT1080 by a multimeric form of the laminin sequence Tyr-Ile-Gly-Ser-Arg (YIGSR). *Br J Cancer* 1996; **73**: 589–595.
26 Lung HL, Bangarusamy DK, Xie D, Cheung AK, Cheng Y, Kumaran MK *et al.* THY1 is a candidate tumour suppressor gene with decreased expression in metastatic nasopharyngeal carcinoma. *Oncogene* 2005; **24**: 6525–6532.
27 Robertson GP, Huang HJ, Cavenee WK. Identification and validation of tumor suppressor genes. *Mol Cell Biol Res Commun* 1999; **2**: 1–10.
28 Li HM, Man C, Jin Y, Deng W, Yip YL, Feng HC *et al.* Molecular and cytogenetic changes involved in the immortalization of nasopharyngeal epithelialcells by telomerase. *Int J Cancer* 2006; **119**: 1567–1576.
29 Brooks PC, Clark RA, Cheresh DA. Requirement of vascular integrin alpha v beta 3 for angiogenesis. *Science* 1994; **264**: 569–571.
30 Avraamides CJ, Garmy-Susini B, Varner JA. Integrins in angiogenesisand lymphangiogenesis. *Nat Rev Cancer* 2008; **8**: 604–617.
31 Urieli-Shoval S, Cohen P, Eisenberg S, Matzner Y. Widespread expression of serum amyloid A in histologically normal human tissues. Predominant localization to the epithelium. *J Histochem Cytochem* 1998; **46**: 1377–1384.
32 Sung HJ, Ahn JM, Yoon YH, Rhim TY, Park CS, Park JY *et al.* Identification and validation of SAA as a potential lung cancer biomarker and its involvement in metastatic pathogenesis of lung cancer. *J Proteome Res* 2011; **10**: 1383–1395.
33 Frisch SM, Screaton RA. Anoikis mechanisms. *Curr Opin Cell Biol* 2001; **13**: 555–562.
34 Glaser R, Zhang HY, Yao KT, Zhu HC, Wang FX, Li GY *et al.* Two epithelial tumor cell lines (HNE-1 and HONE-1) latently infected with Epstein–Barr virus that were derived from nasopharyngeal carcinomas. *Proc Natl Acad Sci USA* 1989; **86**: 9524–9528.
35 Huang DP, Ho JH, Poon YF, Chew EC, Saw D, Lui M *et al.* Establishment of a cell line (NPC/HK1) from a differentiated squamous carcinoma of the nasopharynx. *Int J Cancer* 1980; **26**: 127–132.
36 Cheung ST, Huang DP, Hui AB, Lo KW, Ko CW, Tsang YS *et al.* Nasopharyngeal carcinomacell line (C666-1) consistently harbouring Epstein–Barr virus. *Int J Cancer* 1999; **83**: 121–126.
37 Tsang CM, Zhang G, Seto E, Takada K, Deng W, Yip YL *et al.* Epstein–Barr virus infection in immortalized nasopharyngeal epithelialcells: regulation of infection and phenotypic characterization. *Int J Cancer* 2010; **127**: 1570–1583.
38 Chan KC, Ko JM, Lung HL, Sedlacek R, Zhang ZF, Luo DZ *et al.* Catalytic activity of Matrix metalloproteinase-19 is essential for tumor suppressor and anti-angiogenic activities in nasopharyngeal carcinoma. *Int J Cancer* 2011; **129**: 1826–1837.
39 Venetsanakos E, Mirza A, Fanton C, Romanov SR, Tlsty T, McMahon M. Induction of tubulogenesis in telomerase-immortalized human microvascular endothelial cells by glioblastoma cells. *Exp Cell Res* 2002; **273**: 21–33.
40 Zhang H, Jin Y, Chen X, Jin C, Law S, Tsao SW *et al.* Cytogenetic aberrations in immortalization of esophageal epithelial cells. *Cancer Genet Cytogenet* 2006; **165**: 25–35.
41 Deng W, Tsao SW, Guan XY, Lucas JN, Si HX, Leung CS *et al.* Distinct profiles of critically short telomeres are a key determinant of different chromosome aberrations in immortalized human cells: whole-genome evidence from multiple cell lines. *Oncogene* 2004; **23**: 9090–9101.
42 Lung HL, Lo PH, Xie D, Apte SS, Cheung AK, Cheng Y *et al.* Characterization of a novel epigenetically-silenced, growth-suppressive gene, ADAMTS9, and its association with lymph node metastases in nasopharyngeal carcinoma. *Int J Cancer* 2008; **123**: 401–408.
43 Lo PH, Lung HL, Cheung AK, Apte SS, Chan KW, Kwong FM *et al.* Extracellular protease ADAMTS9 suppresses esophageal and nasopharyngeal carcinoma tumor formation by inhibiting angiogenesis. *Cancer Res* 2010; **70**: 5567–5576.
44 Huang Z, Cheng Y, Chiu PM, Cheung FM, Nicholls JM, Kwong DL *et al.* Tumor suppressor alpha B-crystallin (CRYAB) associates with the cadherin/catenin adherens junction and impairs NPC progression-associated properties. *Oncogene* 2012; **31**: 3709–3720.
45 Thorn CF, Whitehead AS. Differential glucocorticoid enhancement of the cytokine-driven transcriptional activation of the human acute phase serum amyloid A genes, SAA1 and SAA2. *J Immunol* 2002; **169**: 399–406.
46 Kumon Y, Suehiro T, Faulkes DJ, Hosakawa T, Ikeda Y, Woo P *et al.* Transcriptional regulation of serum amyloid A1 gene expression in human aortic smooth muscle cells involves CCAAT/enhancer binding proteins (C/EBP) and is distinct from HepG2 cells. *Scand J Immunol* 2002; **56**: 504–511.
47 Ko JM, Chan PL, Yau WL, Chan HK, Chan KC, Yu ZY *et al.* Monochromosome transfer and microarray analysis identify a critical tumor-suppressive region mapping to chromosome 13q14 and THSD1 in esophageal carcinoma. *Mol Cancer Res* 2008; **6**: 592–603.
48 Protopopov AI, Li J, Winberg G, Gizatullin RZ, Kashuba VI, Klein G *et al.* Human cell lines engineered for tetracycline-regulated expression of tumor suppressor candidate genes from a frequently affected chromosomal region, 3p21. *J Gene Med* 2002; **4**: 397–406.
49 Moffat J, Grueneberg DA, Yang X, Kim SY, Kloepfer AM, Hinkle G *et al.* A lentiviral RNAi library for human and mouse genes applied to an arrayed viral high-content screen. *Cell* 2006; **124**: 1283–1298.
50 Sarbassov DD, Guertin DA, Ali SM, Sabatini DM. Phosphorylation and regulation of Akt/PKB by the rictor–mTOR complex. *Science* 2005; **307**: 1098–1101.

51 Lung HL, Cheung AK, Xie D, Cheng Y, Kwong FM, Murakami Y *et al.* TSLC1 is a tumor suppressor gene associated with metastasis in nasopharyngeal carcinoma. *Cancer Res* 2006; **66**: 9385–9392.
52 Yamada T, Kluve-Beckerman B, Liepnieks JJ, Benson MD. Fibril formation from recombinant human serum amyloid A. *Biochim Biophys Acta* 1994; **1226**: 323–329.
53 Wong VC, Chen H, Ko JM, Chan KW, Chan YP, Law S *et al.* Tumor suppressor dual-specificity phosphatase 6 (DUSP6) impairs cell invasion and epithelial-mesenchymal transition (EMT)-associated phenotype. *Int J Cancer* 2012; **130**: 83–95.
54 Mould AP. Analyzing integrin-dependent adhesion. *Curr Protoc Cell Biol* 2011. (Chapter 9), Unit 9.4.1–9.4.17.
55 Perron-Sierra F, Saint Dizier D, Bertrand M, Genton A, Tucker GC, Casara P. Substituted benzocycloheptenes as potent and selective alpha(v) integrin antagonists. *Bioorg Med Chem Lett* 2002; **12**: 3291–3296.
56 Treuting, PM Dintzis, SM Frevert, CW Liggitt, HD Montine, KS. *Comparative Anatomy and Histology: A Mouse and Human Atlas*, 1st edn. Elsevier/Academic Press: Amsterdam, Netherlands/Boston, MA, USA, 2012.

Supplementary Information accompanies this paper on the Oncogene website (http://www.nature.com/onc)